

SIMULATION OF THE GENERATION AND TRANSPORT OF LASER-ACCELERATED ION BEAMS

O. Boine-Frankenheim, L. Zsolt, TU Darmstadt, Germany
V. Kornilov, GSI, Darmstadt, Germany

Abstract

In the framework of the LIGHT project a dedicated test stand is under preparation at GSI for the transport and focusing of laser accelerated ion beams. The relevant acceleration mechanism for the parameters achievable at the GSI PHELIX laser is the TNSA (Target Normal Sheath Acceleration). The subsequent evolution of the ion beam can be described rather well by the isothermal plasma expansion model. This model assumes an initial dense plasma layer with a 'hot' electron component and 'cold' ions. We will present 1D and 2D simulation results obtained with the VORPAL code on the expansion of the beam and on the cooling down of the neutralizing electrons. The electrons and their temperature can play an important role for the focusing of the beam in a solenoid magnet, as foreseen in the GSI test stand. We will discuss possible controlled de-neutralization schemes using external magnet fields.

INTRODUCTION

The acceleration of ions with lasers up to energies of 60 MeV has been successfully demonstrated at different laser systems worldwide. The intense ($> 10^{19}$ W/cm²) and short (< ps) laser pulse impinges on a thin (μm) metal foil. The laser heats the target electron to temperatures in the MeV range. The hot electrons form a sheath at the rear side of the target and the ions are accelerated in the space charge field formed by the hot electron sheath. This is the TNSA (Target Normal Sheath Acceleration) mechanisms [1]. Simulation studies indicate that higher beam energies (> 100 MeV) can be reached with alternative mechanisms, like the RPA (Radiation Pressure Acceleration) [2]. The experiments and simulations usually focus on the ion energy spectrum and the divergence of the ion beam immediately behind the target. In the TNSA regime the divergence is usually of the order of few degrees and the energy spectrum is well represented by an exponential distribution. The beam is usually assumed to be neutralized by co-moving electrons. For possible applications, e.g. in cancer therapy [3], the ion beam must be focused and transported over distances of several meters. At GSI a pulsed solenoid magnet placed about 10 cm behind the target is used to focus and to collimate protons accelerated by the PHELIX laser system [4]. Proton beams with up to 10^{12} particles and energies around 2.3 MeV to 5 MeV could be collimated, transported and detected along a distance of more than 30 cm. In the framework of the LIGHT project it is foreseen to add a 2.5 m long drift section and a rf buncher cavity. The solenoid will then be used to focus different energies into the RF cavity. The experimental program is

supported by combined simulation studies of the laser ion acceleration and the interface to the conventional beam optics elements. Of great importance is an accurate knowledge of the initial beam distribution (ions and electrons) at the entrance of the collimation section. The simulations are complicated by the large variation of the time and length scales from the laser target through the transport sections. Briefly one distinguishes the following phases with the length and time scales given in brackets

1. Laser target-interaction and electron heating (μm , fs)
2. Expansion and drift of the beam (mm, ps)
3. Beam collimation and de-neutralization in the solenoid (cm, $\mu\text{s}/100$)
4. Conventional ion optics (m, μs)

The different phases or scales require different simulation approaches with clear recipes for the transition between the numerical approaches. In this contribution we employ the plasma simulation code VORPAL [5] and focus on the first two phases and on the initial beam distribution entering the solenoid.

TNSA AND PLASMA EXPANSION

In the TNSA mechanism the hot electron temperature (T_h) and density (n_h) generated by the laser determines the energy and intensity of the ion beam. The plasma, consisting of cold and hot electrons together with cold ions, expands from the target. Thereby the thermal energy of the hot electrons is transformed into forward energy of the ions. TNSA can be well described in terms of models assuming an expanding plasma layer formed by beam ions and electrons [7]. In the following we will present example results from 1D laser-plasma simulations for a target thickness of $3 \mu\text{m}$ ($= 38\lambda_D$, Debye length λ_D), laser intensity 10^{19} W/cm², pulse duration 115 fs ($= 9/\omega_{pi}$, ion plasma frequency ω_{pi}) and target density of $10n_{cr}$ (n_{cr} critical target density for laser reflection). At the end of the laser pulse (when the electron heating stops) the hot electron temperature is 400 keV and the hot electron density is 16 % of the target density. In Fig. 1 the density profile at the rear side of the target is shown. One can observe a steep jump in the density, which is due to the cold electrons. The dashed line is the analytical solution for an isothermal expansion [6]: $n_e = n_{eh} \exp(-x/c_s t - 1)$. The dashed line drifts to the left with the ion sound velocity $c_s = \sqrt{T_h/m_i}$, which is also the velocity of the rarefaction wave [7]. One important observation is that the expansion and acceleration can be described by a one-temperature expansion with initial plasma density equal to the density of laser-produced hot electron density. In Fig.2 the ion front velocity is shown and we get a good agreement between the simple theory

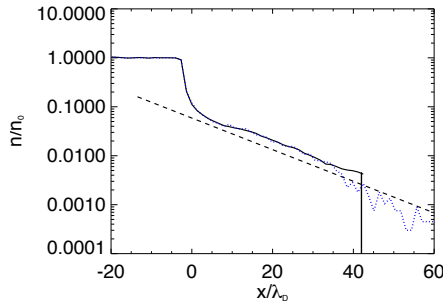


Figure 1: Density profiles of protons (full black line) and electrons (blue dotted) at $\omega_{pi}t = 16$. The position $x = 0$ corresponds to the initial edge of the target and the full thickness is $L_t = 40\lambda_D$.

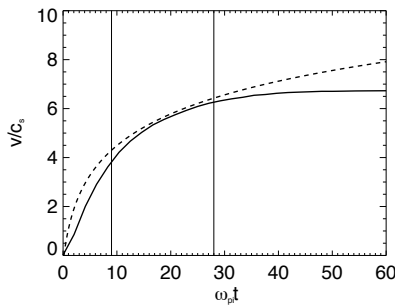


Figure 2: Time evolution of the ion front velocity, full line, and the theoretical prediction, dashed line, from eq. 1. The zero time moment corresponds to the time when the hot electrons reach the target rear surface.

and the simulation, if we use the already mentioned hot electron parameters. The dashed line is a logarithmic function of time [6]:

$$v_{max} = 2c_s \ln(\tau + \sqrt{\tau^2 + 1}), \quad \tau = \frac{\omega_{pi}t}{\sqrt{2}e_N} \quad (1)$$

where $e_N = 2.718$ is the Euler number. The vertical lines represents the borders between the three main phases of TNSA: laser, quasi-isothermal and adiabatic. The acceleration time can be estimates as:

$$\tau_{acc} = \tau_L + \frac{L_{target}}{2c_s} = \tau_L + \tau_{iso} \quad (2)$$

This time is shown by the second vertical line, after this the acceleration stops. The acceleration mechanism in the TNSA is as follows: during the laser pulse the hot electrons are produced, their temperature and density increases until the end of the pulse, then the isothermal phase starts until the rarefaction wave [7] reaches the middle of the target, then the acceleration stops and the adiabatic cooling of the electrons starts. By knowing τ_{acc} we can predict the maximum energy achieved during the TNSA and the final ion energy distribution from the isothermal model [6].

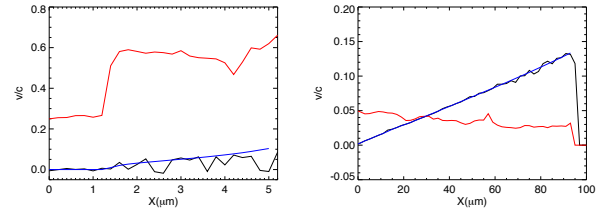


Figure 3: The electron rms velocity (of all electrons) in red at $\omega_{pi}t=18$ (left) and $\omega_{pi}t=236$ (right). In black the mean velocity of electrons is plotted. The blue line represents the proton velocity in space. The $x = 0$ point is the middle of the target.

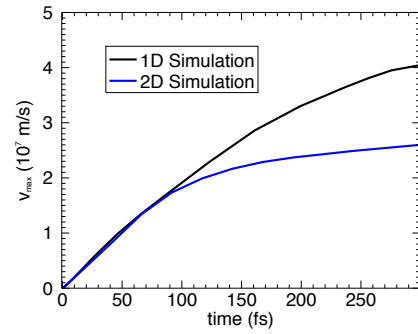


Figure 4: Ion front velocity in 1D (blue line) and 2D case. $t = 0$ corresponds to the time moment when the hot electrons reach the target rear surface.

The agreement is good, but the formulas are valid only in the isothermal phase of the TNSA, after τ_{acc} the energy spectrum remains unchanged. For the subsequent transport of the beam the properties of the neutralizing electrons are important. In Fig. 3 one can see that the hot electrons (left figure) quickly cool down and become co-moving with the ions. From this plot we can conclude that in the case of a simple proton plasma, which contains initially a hot electron population, the final velocity in space and time can be expressed by: $v = x/t$. The electron cooling observed in the simulation follows $T_h \sim t^{-2.6}$, while the adiabatic theory [7] predicts $T_h \sim t^{-2}$. We also performed 2D simulations with the same laser and target parameters. In Fig. 4 we can see that the acceleration is different from the 1D isothermal expansion. The ion front velocity is smaller than the prediction of Eq. 1. 2D and 1D simulations have been performed with the same laser and target parameters. In 2D the laser had a gaussian intensity profile in transverse direction. In Fig. 4 we can see the ion front velocity from the simulations. As we can see the acceleration is the same at the beginning, which is not surprising, because the laser intensity at the axis of symmetry is the same in every moment of time as in 1D. Later the acceleration becomes weaker and quickly stops after the laser pulse, because the hot electrons spread out in transverse direction and disappear from the hot spot. In order to predict the 2D energy

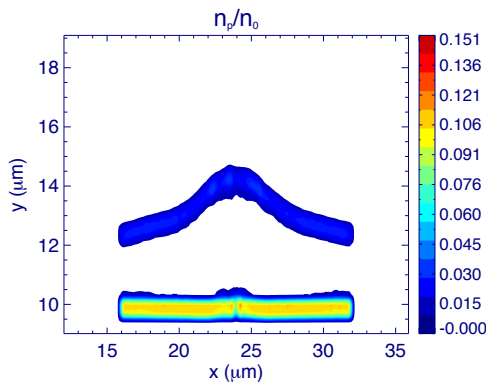


Figure 5: Proton density contour plot at $t = 300 fs$. The target and laser parameters are the same as in Fig. 4, but we applied a $0.1 \mu m$ thick proton layer on the back surface (inside of the target) with $n_0 = 0.01n_t$, n_t is the initial target density.

cutoff for the ions we have to know what happens during the laser pulse. Our observation is that while in 1D the hot electron density and temperature are increasing in time, in 2D we have the opposite case due to the transversal degree of freedom. If we assume that for a time comparable to the laser pulse duration the hot electron Debye length (λ_{Dh}) is larger than the density scale length (L_n), then we can estimate the peak accelerating field with the expression [9]: $E_f = \sqrt{2/e_N} \sqrt{n_h T_h / \epsilon_0}$. This regime can be longer than the pulse duration for heavier ions, because they expand slower. However, the time evolution of the hot electron pressure ($n_h T_h$) is very complicated in case of the proton plasma. We have performed 2D simulations with immobile ions, when the electrons do not lose energy, and the result shows that the peak electric field at the rear surface stays more or less constant during the laser pulse. The approximately constant hot electron pressure at the axis of symmetry is maintained by the heating laser pulse. This more realistic assumption indicates that a recently developed quasi-static theory [10] would describe better the proton acceleration from a heavy-ion target. In the PHELIX experiments a metal target is used with a few hundred nm thick hydrogen-rich contamination layer on its rear surface. In this case the protons can be treated as test particles, because their density is much less than the target density, and they do not perturb significantly the hot electron Debye sheath. One can assume that the heavy ions do not move during the acceleration time of protons, which see a constant accelerating field. In Fig. 5 the detachment of a proton layer from the heavy target. Ongoing work focuses on a comparison of theory [10] and simulation result.

INITIAL DISTRIBUTION FOR BEAM TRANSPORT STUDIES

As an output of this study the initial beam distribution for transport simulations (phase 3 of the multiscale problem)

04 Hadron Accelerators

A14 Advanced Concepts

should be provided. A transport simulation code can use a coarser grid than that of the target interaction code, in order to be able to cover the distance of about 2 m. The expanding plasma flux is injected into the transport code a few mm behind the target at $z = z_*$. The distance z_* should be large enough to ensure that the incoming plasma density is low so that the Debye length can be resolved on the coarser grid and that the electrons are co-moving with the ions. The latter means that no acceleration takes place and ions and electrons are drifting together as a quasineutral plasma. Adopting the results of our 1D simulations, the velocity distribution should be $v_z(z) = c_s + z/t_*$ for $[-c_s t_* < z < z_*]$ such that $v_{max}(\tau_{acc}) = c_s + z_*/t_*$. The density distribution is given by $n(z) = n_* \exp(-z/(c_s t_*)) - 1$ for $[-c_s t_* < z < z_*]$, where the hot electron density at the end of the laser pulse can be used to estimate $n_* = n_{eh}$. The correct divergence (or opening angle) for different ion energies should still be obtained from 2D simulations, as well as the transverse density distribution and the effective source size for different energies. The recipe for a heavy target with a thin proton plasma layer may have differences and should be worked out. The initial distribution discussed here applies to the TNSA mechanism, for other regimes, like RPA, the initial conditions can be very different.

CONCLUSIONS

The ion and electron momentum distributions generated from the TNSA mechanism were studied using 1D and 2D PIC simulations for parameters close to the proton acceleration experiments at the PHELIX laser system at GSI. For a pure proton plasma layer we show that the acceleration process stops after a characteristic time τ_{acc} . In the expanding plasma the hot electrons quickly cool down and can be assumed to be co-moving with the ions. In 2D we observe a shorter acceleration time and a lower maximum ion velocity. Assuming a heavy target with a thin hydrogen layer at the rear side simplifies the analysis considerably. We briefly outline a recipe to construct the initial neutralized beam distribution for transport simulations.

REFERENCES

- [1] S. C. Wilks et al., Phys. Rev. Lett., 69, 1383 (1992)
- [2] T. Esirkepov et al., Phys. Rev. Lett., 92, 175003 (2004)
- [3] I. Hofmann, et al., Phys. Rev. ST Accel. Beams, 14, 31304 (2011)
- [4] K. Harres et al., Phys. Plasmas 17, 023107 (2010)
- [5] <http://www.txcorp.com/products/VORPAL/>
- [6] P. Mora, Phys. Rev. Lett., 90, 185002 (2003)
- [7] P. Mora, Phys. Rev. E, 72, 056401 (2005)
- [8] A. A. Andreev et al., Phys. Plasmas, 10, 220 (2003)
- [9] A. Flacco et al., Phys. Rev. E 81, 036405 (2010)
- [10] M. Passoni, M. Lontano, Phys. Rev. Lett., 101, 115001 (2008)